

THE ELECTROMAGNETIC MODEL OF GAMMA RAY BURSTS

M. LYUTIKOV

University of British Columbia, 6224 Agricultural Road, Vancouver, BC, V6T 1Z1,
Canada

Department of Physics and Astronomy, University of Rochester, Bausch and Lomb
Hall, P.O. Box 270171, 600 Wilson Boulevard, Rochester, NY 14627-0171, USA

Abstract. I describe electromagnetic model of gamma ray bursts and contrast its main properties and predictions with hydrodynamic fireball model and its magnetohydrodynamical extension. The electromagnetic model assumes that rotational energy of a relativistic, stellar-mass central source (black-hole-accretion disk system or fast rotating neutron star) is converted into magnetic energy through unipolar dynamo mechanism, propagated to large distances in a form of relativistic, subsonic, Poynting flux-dominated wind and is dissipated directly into emitting particles through current-driven instabilities. Thus, there is no conversion back and forth between internal and bulk energies as in the case of fireball model. Collimating effects of magnetic hoop stresses lead to strongly non-spherical expansion and formation of jets. Long and short GRBs may develop in a qualitatively similar way, except that in case of long burst ejecta expansion has a relatively short, non-relativistic, strongly dissipative stage inside the star. Electromagnetic and fireball models (as well as strongly and weakly magnetized fireballs) lead to different early afterglow dynamics, before deceleration time. Finally, I discuss the models in view of latest observational data in the Swift era.

1. Short introduction

Gamma Ray Bursts (GRBs) are conventionally divided into two classes, short-hard and long-soft, distinguished by their duration (with a division near ~ 2 sec) and spectrum hardness (Kouveliotou *et al.*, 1993). Detection of Type Ic supernovae nearly coincidence with long GRBs unambiguously linked them with deaths of massive stars (Stanek *et al.*, 2003; Hjorth *et al.*, 2003). Studies of the host galaxies of long GRBs, which turned out to be actively star-forming, further strengthens this association (Djorgovski *et al.*, 1998). Recent progress in observations of short bursts showed that on one hand they show qualitatively similar afterglow behavior (but without any supernovae signature) while on the other hand their energetics was two to four orders of magnitude smaller and they are preferentially (at the moment of writing three out of four) associated with older stellar population (Gehrels *et al.*, 2005; Prochaska *et al.*, 2005; Villasenor *et al.*, 2005; Covino *et al.*, 2005; Retter *et al.*, 2005; Fox *et al.*, 2005). These indirect evidences are consistent with formation of short GRBs in compact star mergers (double neutron stars or black holes–neutron star binaries) and formation of a black hole (*e.g.* Rosswog *et al.*, 2003; Aloy *et al.*, 2005).

2. Short and long GRBs

Association of two types of GRBs with different astronomical objects is somewhat surprising given their apparent similarity (perhaps less surprising in view of the fact that some short GRBs may be associated with nearby SGRs). One possible reason is that though short and long GRBs occur in different astrophysical setting, their appearance is governed by similar physical process related to formation and early evolution of stellar mass relativistic compact object. [Similarities of temporal and spectral properties of the first 2 seconds in long bursts and short bursts (Nakar & Piran, 2002; Ghirlanda *et al.*, 2003) may be an indication of this.] But then one expects that during merger of, *e.g.*, two neutron stars the resulting black hole has large angular momentum and thus can potentially release much more energy than observed (one can invoke different efficiencies, but a naive guess would be that it's harder to extract and propagate energy from a compact object inside a stellar core, contrary to observations).

So why short GRBs are so under-energetic if compared with long ones? One possibility is that presence of a disk is a necessary condition for extracting energy from a black hole, so after disk disappears energy extraction stops. In this case the energy and angular momentum that will power a GRB outflow effectively come not from the central black hole but from the surrounding disk (in a sense that its the energy and/or lifetime of the disk and not the energy in the black hole that determines the resulting energy of a GRB outflow) (for related discussion see also van Putten , 2005).

In case of neutron star mergers, black hole forms fairly early, while the mass of the accretion disk is small, $\leq 0.1M_{\odot}$, with short viscous time scales, $\sim 0.1 - 1$ sec (*e.g.* Ruffert & Janka, 2001). On the other hand, a black hole inside a collapsing core of

a massive star may accrete several solar masses of material (*e.g.* MacFadyen *et al.*, 2001) (at any given moment the mass of the disk is small, but large amount of mass, $\sim 1 - 10M_{\odot}$ passes through the disk during accretion). In addition, amount of the rotational energy stored in case of core collapse depends on core rotation before explosion (which, in turn, depends on metallicity through wind angular momentum loss Woosley & Heger (2005)), resulting in broad spread of rotational energies.

3. Principal issues: electromagnetic and fireball models

In this contribution we describe electromagnetic model of GRBs which assumes that the energy that will power a GRB comes from rotational kinetic energy of a central source. The energy is extracted through magnetic field, which can be generated by a local dynamo mechanisms (*e.g.* De Villiers *et al.*, 2005; Hawley & Krolik, 2005; Proga *et al.*, 2003; McKinney & Gammie, 2004). As argued above, the GRB energy should then be related not to the total rotational energy of a central black hole but to the disk around it. Another possibility for long bursts is formation of a "millisecond magnetar", a fast rotating strongly magnetized proton-neutron star.

Whether magnetic fields play an important dynamical role at any stage in the outflow remains, in our view, one of the principal issues in GRBs physics. Currently, the overwhelming point of view, advocated by the fireball model (FBM) is that magnetic fields do not play any major dynamical role (except, perhaps, at a very early stage; after which fields are dissipated quickly). FBM advocates that in the emission region magnetic fields are re-created locally (*e.g.* through development of Weibel instability (Medvedev & Loeb, 1999)), with energy density typically much smaller than plasma energy density. Fields are small scale, with correlation length l_c much smaller than the "horizon" length $l_c \ll R/\Gamma$ (R is the radius of the outflow in the laboratory frame and Γ is its bulk Lorentz factor). Alternative approach, advocated by MHD and electromagnetic models (*e.g.* Usov, 1992; Blandford, 2002; Lyutikov & Blandford, 2003) is that there are dynamically important large scale fields with "super-horizon" correlation length $l_c \geq R/\Gamma$, which are created at the source and which may play a major role in driving the whole outflow in the first place.

To quantify the dynamical importance of large scale magnetic fields, it is useful to introduce magnetization parameter σ as a ratio of Poynting F_{Poynting} to (cold) particle F_p fluxes (or as a ratio of rest frame energy densities)

$$\sigma = \frac{F_{\text{Poynting}}}{F_p} = \frac{B^2}{4\pi\Gamma\rho c^2} = \frac{b'^2}{8\pi\rho'c^2} \quad (1)$$

where B and ρ are magnetic field and plasma density in the lab frame, b' and ρ' are magnetic field and plasma density in the plasma frame (where electric field is zero). For $\sigma \ll 1$ magnetic fields are dynamically unimportant (this is assumed within a framework of a conventional FBM), while for $\sigma \geq 1$ magnetic fields start to play important dynamical role. For $\sigma \gg 1$, there is an important qualitative change in

the dynamical behavior of the flow at $\sigma_{crit} = \Gamma^2/2$. For $\sigma < \sigma_{crit}$ the flow is super-Alfvénic, while for $\sigma > \sigma_{crit}$ the flow is sub-Alfvénic (and sub-fastmagnetosonic). The difference is somewhat analogous to the difference between sub-sonic and supersonic flows in hydrodynamics.

Thus, depending on the parameter σ three qualitatively different regimes for expansion of the ejecta may be identified, which I will call (i) fireball model (FBM below) $\sigma \ll 1$, (ii) MHD models $1 \leq \sigma < \sigma_{crit}$ and (iii) electromagnetic model (EMM below) $\sigma > \sigma_{crit}$. These three possibilities leads to *a qualitatively different dynamic behavior of flows*. Let us next describe qualitatively main features of the models. (As the FBM and EMM are at the extreme range of σ we discuss those first.) ‡

Fireball model (FBM, e.g. Piran, 2004): The defining characteristic of the FBM is that at intermediate distances (far from the central source but before most energy is transferred to the forward shock) most energy produced by the central source is carried by the bulk motion of ions. In temporal order the transformations of energy are as follows. Initially, the energy that will power the GRB and its afterglow is thermalized near the central source, so that most of it is converted into lepto-photon plasma. This internal energy is then converted to the bulk motion of ions, and reconverted back into internal at internal shocks; at the same time, small scale magnetic fields are generated. The energy of these generated magnetic fields is then used to accelerate leptons via Fermi mechanism to highly relativistic energies §.

Electro-magnetic model (EMM, Lyutikov & Blandford, 2003). The defining characteristic of the electro-magnetic model is that the bulk energy of the flow is carried *subsonically* by magnetic field. In temporal order the evolution of the energy proceeds as follows. The energy that will power a GRB comes from kinetic rotational energy of the central source (millisecond pulsar or BH-disk system). It is then converted to magnetic energy using unipolar inductor (like in pulsars), transported to large distances in a form of strongly magnetized wind and is used to accelerate particle in the emission region. Acceleration of particles is done via magnetic dissipation (not through shocks).

MHD model (e.g. Drenkhahn & Spruit, 2002): In this case most energy is also carried by magnetic field (similar to Lyutikov & Blandford (2003)), but the flow is supersonic, similar to FBM. In the current version (Drenkhahn & Spruit, 2002), magnetic field energy is first converted into bulk motion and then dissipated through internal shocks, similar to FBM. This is, in principle, not necessary, so that magnetic field energy may be dissipated directly into emitting particles, similar to EMM.

The principal differences between EMM and MHD approaches is that MHD-type outflow usually cross fast magnetosonic critical surface after which moment they become causally disconnected from their source (Goldreich & Julian, 1970). Initially the flow

‡ Definitions and discussion below is based not on the nature of the central object but on ejecta content at large distances from the central region and before production of γ -rays occurs.

§ The energy that goes to non-thermal particles is *electro-magnetic* even in the FBM: Fermi-type acceleration is done by turbulent EMF associated with fluctuations of magnetic field

is expanding freely, so that the flow dynamics is determined by the internal structure of the flow. Only after the flow reaches the terminal velocity, the interaction with the mediums becomes important. Unlike MHD, force-free flows are sub-fastmagnetosonic so no conditions at the fast critical surface appear. In this case it is the *interaction with boundaries that determines the properties of the flow* (similar to subsonic hydrodynamic flows). Thus, the distinctive feature between MHD and force-free flows is whether the wind becomes fast supersonic (MHD regime, $\sigma < \sigma_{crit}$) or not (force-free regime, $\sigma > \sigma_{crit}$). This important difference leads to somewhat different dynamics of the flow and can be tested with observations, as discussed in §10.2.

4. Source Formation and Energy Release in EMM

4.1. Electromagnetic luminosity and currents

In this section I will describe main ingredients of the EMM, stressing its principal difference and predictions from the FBM. EMM assumes that the GRB “prime mover” is relativistic, fast rotating, near stellar-mass source. As discussed above, in order to reconcile energies of short and long GRBs the “prime mover” should be not the black hole but the disk around it. For numerical estimates I will assume that a central source generates luminosity $L = L_{50} \times 10^{50}$ erg/s for a time t_s , where $t_s \sim 100$ s for long bursts and $t_s \sim 1$ s for short ones (there are indications that both long and short bursts are powered by the same luminosity, but for different time (Fox *et al.*, 2005)). The mass of the central source is $\sim 0.01M_\odot$ for short bursts and $\sim M_\odot$ for long bursts (we stress again that this is the total mass passing through the disk, not in the black hole). The source is assumed to rotate with a spin frequency \sim kHz. In addition, it is assumed that a source possesses a large magnetic field of $B_s \sim 10^{14}L_{50}^{1/2}$ G. If initially the core is fast rotating (*e.g.* Woosley & Heger, 2005), the total rotational energy in the disk, $\sim M_{disk}R_{disk}^2\Omega^2$, in case of core collapse is much larger, $\sim 7.9 \times 10^{52}(M_{disk}/M_\odot)(R_{disk}/\times 10^6\text{cm})^2(\Omega/6.28 \times 10^3\text{rad/s})^2$ erg, than in the case of mergers, $\sim 7.9 \times 10^{50}$ erg with $M_{disk} \sim 0.01M_\odot$ in the above estimate. The source is expected to be active for $t_s \sim E/L \sim 100$ s for longs and ~ 1 s for shorts.

Rotational energy of the central object is extracted by magnetic fields through unipolar induction mechanism, similar to prevailing model of AGN jets (*e.g.* Ferrari, 2004). Magnetic fields both launches the jet (*e.g.* through Blandford-Znajek mechanism) and collimates it by hoop stresses. Latest full relativistic MHD numerical simulations of accretion disk–black hole systems do show formation of the strongly-magnetized axial funnel (*e.g.* De Villiers *et al.*, 2005; McKinney & Gammie, 2004). Thus, *large scale, energetically dominant magnetic fields may be expected in the launching region of GRB jets.*

Qualitatively, in the immediate vicinity of the source, the plasma is separated into two phases: an internal matter-dominated phase in which large currents are flowing and external magnetically dominated phase. Strong magnetic fields and magnetic flux

are generated in the dense medium (a disk or a differentially rotating neutron star-like object), while relativistic outflow is generated in the magnetically dominated phase. In this case matter loading may be expected to be small (*e.g.* analogous to pulsar wind). As the source remains active for \sim thousand to million dynamical times the flow will be able to settle down quickly to a quasi-steady state evolving slowly as the hole or neutron star slows down. The separation into matter- and magnetic field-dominated phases is somewhat similar to the Sun, where dynamo operates in tachocline, deep below the surface, while magnetic energy, and most importantly magnetic flux, are dissipated outside the star.

The key assumption of the model is that the dissipation rate at the source remains low enough so that the power continues to be dominated by the electromagnetic component (rather than the heat of a fireball) well out into the emission region. Thus, electrical currents flows all the way out to the expanding blast wave, rather than been dissipated close to the source. For electromagnetically dominated outflows the value of the total current may be related to the total luminosity of the source

$$I \sim \sqrt{\frac{Lc}{4\pi}} \sim 3 \times 10^{20} L_{50}^{1/2} \text{ A}, \quad (2)$$

where notation $X_n = (X/10^n)$ was adopted. Under general electromagnetic and relativistic conditions the total impedance of the source and the emission region is close to the impedance of free space $\mathcal{Z} \sim 100 \Omega$

In case of long burst, associated with collapse of massive stars, the source will initially inflate a non-relativistically expanding electromagnetic bubble inside the star. This magnetized cavity is separated from the outside material by the (tangential) contact discontinuity (CD) containing a surface Chapman-Ferraro current. This current terminates the magnetic field and completes the circuit that is driven by the source. On a microphysical level the current is created by the particle of the surrounding medium completing half a turn in the magnetic field of the bubble, so that the thickness of the current-carrying layer is of the order of ion gyro-radius. After the break out the density that controls the ejecta expansion falls down, so that expansion becomes relativistic. In case of short burst, associated with merger of two neutron stars, a somewhat similar process will happen, except that there is no non-relativistic stage, so that the bubble is directly inflated in the circumburst medium.

4.2. Distribution of current in the wind: structured jet

The form of expanding bubble depends on lateral distribution of source luminosity, which within a framework of EMM mode is given by lateral distribution of current. At relativistic stage expansion is nearly ballistic (Shapiro, 1979) while at a non-relativistic stage inside a star a flow may be collimated both through the action of magnetic hoop stresses *and* interaction with the surrounding gas (see §5.2). One particular stationary outflow configuration which captures the essential features of the outflow, is that the outgoing current is confined to the poles and the equatorial plane and closes along the

surface of the bubble, Fig. A1. This current distribution minimizes the total energy given a total toroidal magnetic flux and has been advocated in relativistic stationary winds (Heyvaerts & Norman, 2003). The magnetic field in the bubble is inversely proportional to the cylindrical radius, $B_\phi \propto 1/(r \sin \theta)$. Accompanying this magnetic field is a poloidal electrical field so that there is a near radial Poynting flux carrying energy away from the source. Thus, as the magnetic field strength is strongest close to the symmetry axis, the bubble will expand fastest along the polar direction. The internal structure of an outflow then corresponds to a "structured jet" with $L_\theta \sim \theta^{-2}$ (Lipunov *et al.*, 2001; Rossi *et al.*, 2002), so that the central source releases an equal amount of energy per decade of θ .

5. Long GRBs: expansion inside a star

5.1. How important is dissipation?

Some fraction of the central source luminosity is likely to be dissipated close to the source. The fireball model implicitly assumed that all of the energy released is quickly converted into heat, while in the electromagnetic model this does not happen and the energy flows away from the light cylinder mainly in the form of an electromagnetic Poynting flux and the load impedance is located in the emission region.

The issue of dissipation is somewhat complicated as I discuss next. On one hand, somewhat paradoxically, it becomes harder to convert electromagnetic energy directly to pair plasma the stronger the magnetic field becomes. The reason is that the maximum potential drop that is available for dissipation will be limited by various mechanisms of pair production. Typically, after an electron has passed through a potential difference $\Delta V \sim 10^9 - 10^{12}$ V it will produce an electron-positron pair either through the emission of curvature photon or via inverse Compton scattering. This will be followed by an electromagnetic cascade and the newly born pairs will create a charge density that would shut-off the accelerating electric field. Put another way, the pair density required to supply the electrical current and space charge scales linearly with the field strength, while the electromagnetic energy density scales as its square. The stronger the field, the more likely it is to persist into the outflow. It is because GRBs are so powerful that the dissipation in the source is probably low.

There is an important caveat to the preceding discussion which applies to very early, nonrelativistic, stages of bubble expansion in case of long bursts. Somewhat similar to pulsar wind nebulae (*cf.* Rees & Gunn, 1974), *non-relativistic, ideal, homologous expansion of strongly magnetized nebular which is causally disconnected from the source and injects toroidal magnetic field with nearly a speed of light cannot occur.* The reason is that magnetic flux and energy are supplied to the inflating bubble by a rate that cannot be accommodated in the bubble. The rate of supply is determined by the processes inside the light cylinder of a newly-formed, compact object, while inflation of the bubble is controlled by the external gas density. (Even if the wind remains subsonic,

it is unlikely that processes at the edge of the inflating bubble would influence wind generation region near the light cylinder.) This leads to the following "contradiction". Magnetic flux (integrated over the meridional plane) is supplied to the bubble at a rate $\dot{\Phi} \sim 2Ic$. Similarly, energy is supplied to the bubble at a rate $\dot{U}_{\text{EM}} \sim \mathcal{E}I$. We can also compute the magnetic flux $\Phi = \mathcal{L}I$ and the energy stored within the bubble $U_{\text{EM}} = \mathcal{L}I^2/2$, using the self inductance \mathcal{L} . Let the bubble radius be $R(\theta, t)$ where θ is the polar angle measured from the symmetry axis defined by the spin of the compact object. If the magnetic field in the bubble is predominantly toroidal between cylindrical radii ϖ_{min} and $\varpi_{\text{max}} = R \sin \theta$, this is given by

$$\mathcal{L} \sim \frac{\mu_0}{2\pi} \int dz \ln \left(\frac{\varpi_{\text{max}}}{\varpi_{\text{min}}} \right). \quad (3)$$

We therefore see that, if the bubble expands sub-relativistically, the rate of supply of both flux and energy exceeds the rate at which the flux and energy can be stored by a factor $\sim [\ln(\varpi_{\text{max}}/\varpi_{\text{min}})(dz/dt)/c]^{-1}$ (cf. Rees & Gunn, 1974). Therefore, for non-relativistic expansion of the bubble too much flux and too much energy is generated by the source.

The way out of the "paradox" is that dissipation must become important that will destroy some magnetic energy and most importantly eliminate most of the toroidal flux. Most of the dissipation is likely to occur near the axis where the current density is highest and the susceptibility to current-driven instability is the greatest. In this case a lateral flow of energy will set in carrying the poloidal field lines with it towards the axis. This, in turn, will lead to the pile-up of magnetic field near the axis and to faster radial expansion near the axis (the toothpaste tube effect) (Lyutikov & Blandford, 2003).

5.2. Form of the expanding bubble

The dynamics of a non-spherically expanding bubble may be described using the method of Kompaneets (1960). Consider a small section of non-spherical non-relativistically expanding CD with radius $R(t, \theta)$. The CD expands under the pressure of magnetic field so that the normal magnetic stress at the bubble surface is balanced by the ram pressure of the surrounding medium. At the spherical polar angle θ the CD propagates at an angle $\tan \alpha = -\frac{\partial \ln R}{\partial \theta}$ to the radius vector. Balancing the pressure inside the bubble $B^2/(8\pi) = I^2/(2\pi c^2 R^2)$ with the pressure of the shocked plasma gives

$$\left(\frac{\partial R}{\partial t} \right)^2 = \kappa \frac{I^2(t)}{2\pi R^2 \sin^2 \theta \rho(R, \theta)} \left[1 + \left(\frac{\partial \ln R}{\partial \theta} \right)_t^2 \right] \quad (4)$$

where κ is a coefficient of the order of unity which relates the pressure at the CD to the pressure at the forward shock.

Equation (4) shows that non-spherical expansion inside the star is due both to the anisotropic driving by magnetic fields *and* collimating effects of the stellar material (the term in parenthesis, which under certain conditions tends to amplify non-sphericity). The rate of expansion of the bubble inside the star depends upon the density profile of the stellar envelope and the time evolution of the luminosity (or, equivalently, of the

current $I(t)$). For a given dependence $\rho(R, \theta)$ and $I(t)$ Eq. (4) determines the velocity of the CD. Generally solutions will be strongly elongated along the axis. A simple analytical solution for $I, \rho \sim const$ is

$$R(t, \theta) = \left(\frac{2 I^2}{\pi \rho c^2} \right)^{1/4} \frac{\sqrt{t}}{\sin \theta}. \quad (5)$$

(current is related to the luminosity by Eq. (2). Qualitatively, the bubble and the forward shock will cross the iron core ($r_c \sim 2.5 \times 10^8$ cm) in $t \sim r_c \sqrt{\rho} / B(r_c) \sim .3$ sec, short enough to produce an ample supply of ^{56}Ni (Woosley *et al.*, 2003). If $M(R)$ is the stellar mass external to radius R , then the breakout time is

$$t_{\text{breakout}}(\theta) \sim 1\theta_{-1}^2 \left(\frac{M}{M_\odot} \right)^{1/2} \left(\frac{R}{R_\odot} \right)^{1/2} L_{50}^{-1/2} \text{ s} \quad (6)$$

The electromagnetic bubble can be confined equatorially by the star for the duration of the burst $t_{\text{breakout}}(\pi/2) \sim 100$ s and will expand non-relativistically as we have assumed. However the expansion along the axis proceeds on a short time scale and breakout should occur early in the burst.

Thus, along the jet axis non-relativistic expansion lasts for several seconds, which is much shorter than the burst duration. After breakout the flow quickly becomes relativistic so there is no need for dissipation anymore. Thus, relative fraction of dissipated energy is small, so that overall the flow magnetization remains large. Most of the dissipation described above will result in creation of lepto-photonic plasma, which decouples after photosphere, so that the remaining flow remains strongly magnetized. In summary, when the bubble expands non-relativistically, it must be dissipative, while after breakout, the expansion becomes relativistic and the resistance falls so that the electromagnetic energy that is still being supplied by the source is mostly absorbed by the inflating bubble and by doing work against the surroundings.

6. Optically thick expansion: mini-fireball

Under the electromagnetic hypothesis, most of the energy released by the source comes out in the form of Poynting flux. However there must be some dissipation that would lead to creation of a lepto-photonic component (as discussed in §5.1), in case of non-relativistic stage of bubble expansion inside a star dissipation may be considerable). This will create an optically thick "warm" fireball (in a sense that it is dominated by magnetic field energy, but also has considerable pressure). Expansion of this "warm" fireball will create a thermal precursor, similar to the conventional FBM, but modified by presence of magnetic field (Lyutikov & Usov, 2000; Lyutikov & Blandford, 2003).

At early stages (before the breakout in case of long bursts) the plasma enthalpy is strongly dominated by lepto-photonic plasma with a temperature

$$T \sim \left(\frac{L}{a\Delta\Omega r^2 \beta c \Gamma^2 (1 + \sigma)} \right)^{1/4} \quad (7)$$

where $\Delta\Omega$ is a typical opening solid angle and luminosity of the source then can be written as $L = \int d\Omega \Gamma^2 r^2 \beta c (b^2/2 + w)$, where w is plasma enthalpy, b is a toroidal magnetic field in the plasma rest frame times $\sqrt{4\pi}$,

After breakout the flow will accelerate to relativistic velocities. Initially, conical expansion is mostly pressure-driven, even in the strongly magnetized case (in this case magnetic pressure gradients and hoop stresses balance out each other). This results in dynamics qualitatively similar to the unmagnetized case: the wind plasma accelerates $\Gamma \sim r$ while its density, pressure and temperature decrease $n \sim r^{-3}$, $p \sim r^{-4}$, $T \sim r^{-1}$, so that magnetization parameter remains approximately constant (Lyutikov & Blandford (2003)).

When the temperature falls below $\sim 10 - 20 \text{ keV}$, most of the pairs annihilate. This suddenly reduces the optical depth to Thomson scattering below unity. (Under certain conditions photons may remain trapped in the flow. In this case, thermal driving by photon pressure continues, until the thermal photons escape.) As a result the lepto-photon part of the flow decouples from the magnetic field and σ increases by roughly seven orders of magnitude to $\sigma \sim 10^9$. The thermal radiation from the lepto-photon component has a rest-frame temperature $T_0 \sim 10 - 20 \text{ keV}$ times a boost due to the bulk motion. This thermal radiation, which should peak around $\sim 100 \text{ keV}$ may put constraints on the initial σ (Lyutikov & Usov, 2000; Daigne & Mochkovitch, 2002).

7. Relativistic expansion

7.1. Short GRBs and long GRBs after breakout

In case of long GRBs inflating a bubble inside a star, eventually the bubble will break free out of the star forming two axial jets along which Poynting flux will flow until the central source slows down on the time scale $t_s \sim 100 \text{ s}$. Outside the star, the bubble will expand ultra-relativistically and bi-conically. For short GRBs, presumably associated with merger of neutron stars in a low density environment, there is no preceding non-relativistic stage so expansion of the bubble is relativistic from the beginning. In case of relativistic motion there is no necessity anymore to destroy magnetic flux through ohmic dissipation: the effective load can consist of the performance of work on the expanding blast wave. This is where most of the power that is generated by the central magnetic rotator ends up.

After the bubble has expanded beyond a radius $r_{\text{sh}} \sim ct_s \sim 3 \times 10^{12} t_{s,2} \text{ cm}$ ($\sim 10^{10} \text{ cm}$ for short bursts) the electromagnetic energy will be concentrated within an expanding, electromagnetic shell with thickness $\sim r_{\text{sh}}$ and with most of the return current completing along its trailing surface (see Fig. A1). The global dynamics of this shell and its subsequent expansion are set in place by the electromagnetic conditions at the light cylinder and within the collimation region. An important property of ultra-relativistic outflows is that they are hard to collimate (Chiueh *et al.*, 1991; Bogovalov, 2001), so that any collimation should be achieved close to the source, within a star,

where the flow is only mildly relativistic.

Interaction of the magnetic shell with the circumstellar medium proceeds in a similar way to the non-relativistic expansion inside a star: the leading surface of the shell is separated by a contact discontinuity (which actually becomes a rotational discontinuity if the circumstellar medium is magnetized (Lyutikov, 2002a)). Outside the CD an ultra-relativistic shock front forms and propagate into the surrounding circumstellar medium. The expansion is non-spherical. As long as the outflow is ultra-relativistic, the motion of the forward shock is virtually ballistic (Shapiro, 1979) and determined by the balance between the magnetic stress at the CD and the ram pressure of the circumstellar medium.

A type of collimation in case of electromagnetic explosions is somewhat different from the conventional jet models of AGNs. We expect that large Poynting fluxes associated with explosive release of $\sim 10^{51}$ ergs in case of long GRBs are sufficient to drive a relativistic outflow over a large solid angle, so that during the relativistic stage the resulting cavity is almost spherical, but the Lorentz factor Γ of the CD is a strong function of the polar angle. The angular distribution of magnetic field (and of the Lorentz factor of the expansion) depends on the dynamics of the bubble at the non-relativistic stage and the distribution of the source luminosity.

In the framework of electromagnetic model the outflow is strongly magnetized and *subsonic*, $\sigma > \sigma_{crit}$, despite been strongly relativistic. In this case the ejecta, in some sense, may be considered as a collection of outgoing fast magnetosonic waves propagating from the source to the contact discontinuity. Motion of the CD is then determined by the pressure balance between the Poynting flux from the source and the ram pressure of the ISM. Thus, motion of the CD depends on the source luminosity $L(t')$ at the retarded time t' such that $R(t) = t - t'$. In addition to forward flux, there is a much weaker, by a factor Γ^2 , reflected flux that propagates backward into the flow the information about the circumstellar medium. Interference of forward and backward propagating waves allows to define a finite Lorentz factor of the ejecta. The distribution of reflected current is determined by the outgoing current and the boundary conditions. At later times multiple reflections from the contact discontinuity and the center become important as well.

7.2. Stages of relativistic expansion of electromagnetic shell

Relativistic expansion of the magnetized shell may be separated into two stages, which we will call "early" and "late", depending on whether or not most of the fast waves emitted by the central source have caught up with the CD and their energy has been given to the circumburst medium. The transition between two stages occurs at the moment which is similar to the deceleration radius in fireball model, except that in the case of EMM the shell is decelerating all the time, but with different laws before and after the transition. Keeping with the tradition we will still call the transition radius as deceleration radius.

7.2.1. “Early” stage. At $r > r_{ph}$ the outflow becomes a relativistically expanding shell of thickness $\sim ct_s \sim 3 \times 10^{12}$ cm for long GRBs and $\sim 3 \times 10^{10}$ cm for short GRBs. The shell contains toroidal magnetic field; the current now detaches from the source and completes along the shell’s inner surface. At this stage the CD is constantly re-energized by the fast-magnetosonic waves propagating from the central source. The average motion of the CD $R(t)$ is determined by the average luminosity at the retarded time t' :

$$L_\Omega(t') \sim \rho c^3 \Gamma^4 R(t)^2 \beta^3 \quad (8)$$

which for constant luminosity gives $\Gamma \sim (L_\Omega/\rho c^3)^{1/4} r^{-1/2}$ (in a constant density medium) or $\Gamma \sim (L_\Omega/4\kappa\rho_0 r_0^2 c^3)^{1/4} = \text{const}$ (in a $\rho(r) = \rho_0(r_0/r)^2$ wind). If the central source releases most of the current along the axis and the equatorial plane, as argued in §4.2, then $\Gamma \propto 1/\sqrt{\sin\theta}$ at this stage. If source’s luminosity varies, this will be reflected in the “jitter” of the CD. Development of instabilities at the CD, like impulsive Kruskal-Schwarzschild instability (Lyutikov & Blandford, 2003) may lead to dissipation and particle acceleration. The internal structure of the magnetic shell is a messy mixture of the outgoing waves from the source and the ingoing waves reflected from the CD, similar to a pre-Sedov phase in hydrodynamical explosions. Unlike the case of a hydrodynamic blast wave with energy supply, no internal discontinuities form inside magnetic shell.

Early stage lasts for $ct_s < r < r_{\text{dec}}$, where

$$r_{\text{dec}} = (L_\Omega t_s^2/\rho c)^{1/4} \sim 3 \times 10^{16} L_{50}^{1/4} t_s^{1/2} n^{-1/4} \text{cm}, \quad (9)$$

for long bursts (in the observer frame this phase lasts $\sim t_s \sim 100$ s) and $r_{\text{dec}} \sim 3 \times 10^{15}$ cm for shorts (similarly, in the observer frame this phase lasts $\sim t_s \sim 1$ s). Radius r_{dec} (9) is somewhat similar to the deceleration radius in case of FBM; at this moment most energy of the shell is given to the circumburst medium, $L_\theta t_s \sim E(\theta) \sim \rho c^2 r_{\text{dec}}^3 \Gamma(r_{\text{dec}}, \theta)^2$ (note that here $\Gamma = \Gamma(r_{\text{dec}})$, not Γ_0 as in case of FBM, since there is no formal definition of Γ_0 in case of EMM).

7.2.2. “Late stage” ($r_{\text{dec}} < r < r_{\text{NR}} \equiv (L_\Omega t_s/\rho c^2)^{1/3}$). At distances $r > r_{\text{dec}}$ most of the waves reflected from the CD have propagated throughout the shell, so that all the regions of the shell come into causal contact. Most of the energy of the explosion will reside in the blast wave which will eventually settle down to follow a self-similar expansion. As the expanding shell performs work on the surrounding medium its total energy decreases; the amount of energy that remains in the ejecta shell during the late stage is small, $\sim E_\Omega/\Gamma^2$. Most of the energy is still concentrated in a thin shell with $\Delta R \sim R/\Gamma^2$ near the surface of the shell which is moving according to $\Gamma \sim \sqrt{E_\Omega/\rho c^2} r^{-3/2}$ (in a constant density medium), or $\Gamma \sim r^{-1/2}$ (in a $\rho \sim r^{-2}$ wind). If the central source releases most of the current along the axis and the equatorial plane, as discussed in §4.2, then $\Gamma \propto 1/\sin\theta$ at this stage. [Note that at the “early stage” $\Gamma \propto 1/\sqrt{\sin\theta}$, but no lateral re-distribution of energy is required at the transition since transition between “early” and “late” stages occur at different times for different θ .] The energy of the shell decreases only weakly with radius, $dE/dt \sim 1/r$ in constant density and $dE/dt \sim 1/r^3$ in a wind, so that the

surface of the shell keeps moving relativistically as long as the preceding shock wave is moving relativistically, until $r \sim (E_\Omega/\rho c^2)^{1/3} \sim 10^{18}$ cm - the shock never becomes completely free of the shell (Lyutikov & Blandford, 2003). Interestingly, the structure of the *magnetic* shell (in particular the distribution of energy) resembles at this stage the structure of the *hydrodynamical* relativistic blast wave (Blandford & McKee, 1976). This can be formally understood by noting that for motion perpendicular to magnetic field dynamical equations for magnetized flow can be reduce to non-magnetic case, but with a different equation of state (Landau & Lifshits, 1982).

”Late stage” of magnetic shell expansion corresponds to the conventional afterglow phase when synchrotron and inverse Compton radiation is emitted throughout the electromagnetic spectrum. The initially aspheric expansion will give the appearance of a jet with the “achromatic break” occurring when the fastest Lorentz factor of the spine $\Gamma(\theta = 0)$ becomes comparable with the reciprocal of the observer’s inclination angle with respect to the symmetry axis, $\Gamma(\theta = 0) \sim 1/\theta_{ob}$. When $r > r_{NR} \sim (Lt/\rho c^2)^{1/3} \sim 2 \times 10^{18} L_{50}^{1/3} t_{s2}^{1/3} n^{-1/3}$ cm, the blast wave become non-relativistic and will become more spherically symmetric, while evolving towards a Sedov solution.

8. Production of GRB

By the time the shell radius expands to r_{dec} most of the electromagnetic Poynting flux from the source will have caught up with the CD and been reflected by it, transferring its momentum to the blast wave. Simultaneously a strong region of magnetic shear is likely to develop at the *outer* part of the CD (Lyutikov, 2002a).

We propose that the *γ -ray-emitting electrons are accelerated near $r_{dec} \sim 10^{15} - 10^{16}$ cm (for long bursts) and $\sim 10^{15}$ cm (for short bursts) due to development of electromagnetic current-driven instabilities* (conventional model of particle acceleration - acceleration at internal shocks - cannot work in this model since in the limit $\sigma \gg 1$ fast shocks are either weak or do not form at all). The development of current instabilities usually results in enhanced or anomalous plasma resistivity which leads to an efficient dissipation of the magnetic field. The magnetic energy is converted into heat, plasma bulk motion and, most importantly, into high energy particles, which, in turn, are responsible for the production of the prompt γ -ray emission. The conversion of magnetic energy into particles may be very efficient. For example, recent RHESSI observations of the Sun indicate that, in reconnection regions, most magnetic energy goes into non-thermal electrons (Benz *et al.*, 2003).

To illustrate how magnetic dissipation may proceed, we describe shortly physics underlying the development of the so-called tearing mode. Consider a smooth distribution of electrical current, which can be viewed as a set of many small current wires. Since parallel currents attract, such a system is likely to develop narrow current sublayers where dissipation, which is inversely proportional to the square of magnetic field gradient, becomes high. In addition, high anomalous resistivity, proportional to local current density is likely to develop. Similar to non-relativistic plasmas, in strongly

magnetized plasmas tearing mode develops on time scales *much shorter than resistive time scale in the bulk* (Lyutikov, 2003). The final outcome of the development of the tearing mode is formation of reconnection sites and dissipation of magnetic energy.

Particle acceleration by dissipative magnetic fields may proceed in a number of ways. The best studied non-relativistic example is particle acceleration in reconnection regions either by inductive electric fields outside the current sheet or resistive electric fields inside the current sheets (*e.g.* Craig & Litvinenko, 2002) or formation of shocks in the downstream of reconnection regions (*e.g.* Blackman & Field, 1994). Investigation of the particle acceleration in the relativistic regime of reconnection is only beginning (*e.g.* Larrabee *et al.*, 2002). Relativistic reconnection may produce power-law spectra of accelerated particles (Zenitani and Hoshino, 2004; Larrabee *et al.*, 2002). For example, in the relativistic Sweet-Parker reconnection model (Lyutikov & Uzdensky, 2003), if one balances linear acceleration inside the reconnection layer by the resistive electric field, $d_t \mathcal{E} \sim e E c$ with the rate of particle escape (proportional to relativistic gyro-frequency), $d_t \ln N(\mathcal{E}) \sim \omega_B (mc^2/\mathcal{E})$, one finds $N(\mathcal{E}) \sim \mathcal{E}^{-\beta_{in}}$ where \mathcal{E} is the energy of a particle, $N(\mathcal{E})$ is the particle number and β_{in} is the inflow velocity (Zenitani and Hoshino, 2004). For relativistic reconnection the inflow velocity can be relativistic (Lyutikov & Uzdensky, 2003), $\beta_{in} \rightarrow 1$. The fact that reconnection models can produce spectra which are prohibitively hard for shock acceleration may serve as a distinctive property of electromagnetic models.

In addition to the acceleration mechanisms which are based on known non-relativistic schemes, it is feasible that acceleration in relativistic, strongly magnetized plasma may proceed through mechanisms that do not have non-relativistic or fluid analogues. Examples of this type of acceleration include particle acceleration through formation of a spectral cascade of nonlinear waves in force-free plasma which transfer energy to progressively larger wave vectors until this energy is taken up in accelerating a population of relativistic electrons and positrons Thompson & Blaes (1998). Since for $\sigma > 1$ cascade is likely to be terminated at plasma frequency, which is lower by a factor $\sqrt{\sigma}$ the cyclotron frequency, the likely emission mechanism in this case is inverse Compton scattering. Another possibility is development of kinetic electromagnetic-type instabilities of the shell surface currents, as proposed by Smolsky & Usov (1996) and in somewhat different form by Liang *et al.* (2003). Since studies of kinetic properties of strongly magnetized relativistic plasmas are only beginning, it is hard to predict acceleration efficiency and particle spectra. Numerical studies in the coming years will be most important here.

9. Production of afterglows

Except at early stage (as discussed in §7.2.1), afterglows are generated in a similar way both in the FBM and EMM. As the magnetic shell expands, its energy is gradually transferred to the preceding forward shock wave. Relativistic particles are accelerated in the blast wave producing the observed afterglow in a manner which is

similar to what is proposed for fluid models, except that contact discontinuity itself may be an important source of magnetic flux through impulsive Kruskal-Schwarzschild instability (Lyutikov & Blandford, 2003), so that afterglows may result from a mixture of relativistic particles, derived from the shock with magnetic field derived from the shell.

At late times, well beyond r_{dec} (which in observer frame is nearly coincident with the prompt phase), the temporal behavior of proper afterglow (as opposed to tails of prompt emission, see §10.3) is determined by the total energy release E_{Ω} and not by the form of that energy. As a consequence, late afterglow observations can hardly be used to distinguish between the models. The only property of the source that the forward shock "remembers" at late times is the angular distribution of the deposited energy $E(\theta)$ (there is little sideways evolution in relativistic regime (Shapiro, 1979)). Thus, the angular distribution of the total energy $E(\theta)$ can be used to distinguish between different models, if a model predicts it.

In case of EMM, the preferred lateral distribution of the magnetic field, energy fluxes and luminosity correspond to the line current, §4.2, so that $L \sim 1/\sin^2 \theta$. This translates into distribution of Lorentz factors of the forward shock

$$\Gamma \sim \left(\frac{E}{\rho_{\text{ex}} c^5} \right)^{1/2} \frac{t^{-3/2}}{\sqrt{\theta^2 + \theta_0^2}} \quad (10)$$

where θ_0 is the angular size of the core of the jet. (Its minimal size is magnetic Debye radius, $r_D = \sqrt{\frac{I}{2\pi n e c}}$, which gives $\theta_0 \sim \left(\frac{m^2 c^5 \sigma^2 \Gamma^2}{L e^2} \right)^{1/4} \approx 10^{-3} L_{50}^{-1/4} \sigma_9^{1/2} \Gamma_2^{1/2}$, (Lyutikov & Blandford, 2003).) This type of shock has been named "structured jet" (or universal jet) (Lipunov *et al.*, 2001; Rossi *et al.*, 2002), though in our model there is no proper "jet", but simply a non-spherical outflow. The most intense bursts and afterglows in a flux-limited sample will be seen pole-on and can exhibit achromatic breaks when $\Gamma \sim \theta^{-1}$, which might be mistaken for jets.

In conclusion, observational appearance of GRB afterglows depends mostly on two parameters: (i) explosion energy (more precisely, on the ratio on the explosion energy to circumstellar density) and (ii) the viewing angle that the progenitor's axis is making with the line of sight. This possibility, that all GRBs (and XRFs) are virtually the same but viewed at different angles resembles unification scheme of AGNs.

10. Tests of GRB models

10.1. Testing the fireball model: reverse shock emission

Perhaps the simplest test of GRB models could have come from observations of emission from the reverse shock propagating in the ejecta, which typically falls into the optical range. FBM predicts strong reverse shock emission, so that absence of nearly contemporaneous optical emission in most GRBs would be a strong argument against FBM. In MHD models with $\sigma > 1$ reverse shock is weak, while in EMM reverse shock is absent altogether.

Since possible observation of reverse shock emission may play a decisive role in validating a GRB theory, next we discuss briefly properties of the reverse shock expected *within a framework of FBM* (for more extensive discussion see, *e.g.* Sari & Piran, 1999; Kobayashi, 2000). In the framework of FBM both reverse shock and internal shocks which produce prompt γ -ray emission originate in the same fluid and have similar properties (*e.g.* being weakly relativistic). One can naturally expect that microphysical properties of particle accelerating, being complicated and poorly understood, are the same for the same type of shocks. Thus, the conventionally introduced quantities like ϵ_B (magnetic field value with respect to equipartition), ϵ_e (electron energy density with respect to equipartition), and γ_{min} (minimum Lorentz factor of accelerated electrons) *must be the same for both cases*. As a result, for any given burst, observations of the prompt emission can be used to predict properties of a corresponding optical flash.

The amount of energy dissipated in reverse shock is comparable to the energy dissipated in the forward shock and to the total GRB energy (Sari & Piran, 1999). The principal difference between prompt and optical emitting electrons is the radii of emission and ratio of cooling to expansion time scales. In a framework of FBM, prompt emission is generated at distances $r_{GRB} \sim 2\Gamma_0^2 \delta t c \sim 10^{12} - 10^{13}$ cm ($\delta t \sim 0.01$ s is variability time scale of the central source and, within a framework of FBM, of the prompt emission), while reverse shock emission is typically generated at distances $R \sim 2ct_s \Gamma_0^2 \sim 10^{16}$ cm (seen at observer time $t_{obs} \sim t_s$; we concentrate on a simple so called "thick shell" case). Using conventional fireball parameterization for minimum Lorentz factor of accelerated particles $\gamma_{min} \sim \epsilon_e (m_p/m_e) \Gamma_s$ where Γ_s is the shock Lorentz factor, and parameterizing energy density of magnetic field in the plasma rest frame to ion energy density, $\rho c^2 = L/(4\pi\Gamma_0^2 r^2 c)$ and $b = \sqrt{\epsilon_B} \sqrt{8\pi\rho c^2}$, the ratio of prompt to reverse shock frequencies is

$$\frac{\omega_{GRB}}{\omega_{RS}} \sim \frac{r_{RS}}{r_{GRB}} \left(\frac{\Delta\Gamma}{\Gamma_{RS}} \right)^2 \sim \frac{r_{RS}}{r_{GRB}} \sim \frac{t_s}{\delta t} \quad (11)$$

so that the peak of reverse shock emission occurs at $\sim 1 - 10$ eV.

An important qualitative difference between prompt and optical emitting electrons is that the former are in fast cooling regime, while the latter are in slow cooling regime. The radius beyond which optically emitting electrons enter slow cooling regime,

$$r_{cool} \sim \epsilon_B \epsilon_e \frac{(\Gamma_{RS} - 1) L m_p \sigma_T}{3\pi c^3 m_e^2 \Gamma_0^3} \sim 2 \times 10^{14} L_{50\text{cm}}, \quad (12)$$

($\Gamma_{RS} - 1 \sim 1$ and $\Gamma_0 = 300$ was assumed) is typically smaller than R_{RS} . As result, only small fraction of energy received by an optical electron $\sim R_{RS}/(\Gamma_0 r_{cool}) \sim 0.02$ is emitted; the rest is lost to adiabatic expansion. For a GRB of $E_\gamma \sim 10^{51}$ ergs, optical flash would have $E \sim 10^{49}$ ergs. For a typical GRB burst with fluency $\sim 10^{-6}$ erg/cm², and duration of ~ 100 sec, this will result in optical flash of magnitude $\sim 12m$. Even if we increase the estimate of R_{RS} and duration of optical flash each by an order of magnitude, resulting optical flash would have $\sim 17m$. On the other hand, brightest bursts may reach fluences $\sim 10^{-4}$ erg/cm², which, according to these estimates, can

produce optical flash of $\sim 7m$. In addition, adiabatic cooling results in flux decay $\propto t^{-2}$ and a clear radio signal is expected (*e.g.* Nakar & Piran, 2004). Thus, fireball model makes a predictions that all GRBs must have optical flashes in the range $12m-17m$, with some variations of few magnitudes (both brighter and dimmer) depending on particular properties of each burst.

In the Swift era, *not a single GRB has shown the predicted behavior*. This is despite the fast on-board optical telescope and a large number of ground based robotic telescopes (RAPTOR, ROTSEE, TAROT and others). *Reverse shock emission is virtually an unavoidable prediction of the fireball model, so that absence of predicted reverse shocks emission in the Swift era argues against the fireball model*. Naturally, there is a number of ways that through which optical flashes can be suppressed (*e.g.* cooling of optically emitting electrons on photons of prompt emission Beloborodov (2002), "thin shell case", when the reverse shock emission is spread over longer times, producing weaker signal (*e.g.* McMahan *et al.*, 2005)). *A possible explanation of an absence of clear reverse shock signal is that ejecta plasma is strongly magnetized*. In the case when energy density of magnetic field dominates the total energy density ($\sigma \geq 1$) reverse shock becomes very inefficient in dissipating flow energy (Kennel & Coroniti, 1984).

Irregular optical flashes (like GRB 050525a (Klotz *et al.*, 2005) and GRB 050904 (Boër *et al.*, 2005)) may be produced by other mechanisms, like gamma-ray pair production in front of the forward shock, Beloborodov (2002); Thompson & Madau (2000), or be a low energy tail of prompt emission.

10.2. Electromagnetic model: bright early afterglows

Fireball and electromagnetic models make very different prediction for the properties of early afterglows (see Fig. A2, Lyutikov, 2004). According to EMM, at the early afterglow stage the Lorentz factor and peak frequency are larger (and falling with time) than in the FBM (constant Lorentz factor and peak frequency). *Early afterglow in the EMM are more energetic than in FBM*, Fig. A3, and can blend with the prompt phase.

10.3. Emission radius of prompt photons and early Swift afterglows

One of the surprising early results from Swift satellite was detection of X-ray spikes and breaks in light curves at intermediate times, much longer than burst duration but well before the conventional jet break (*e.g.* Tagliaferri *et al.*, 2005; Nousek *et al.*, 2005; Chincarini *et al.*, 2005). A typical behavior includes fast-slow-fast decay with transitions near $100 - 1000$ seconds and $\sim 10^4$ seconds. This presents a real challenge to GRB models, since if the emission is seen "head on", within angle $\theta \leq 1/\Gamma$, the radii at which these features should be produced correspond to radii much larger than deceleration radius. At these times most of the energy is in the forward shock which should produce smooth light curve. (Late time injection or specific distribution of Lorentz factors are some possibilities discussed (*e.g.* Zhang *et al.*, 2005; Lazzati & Begelman, 2005). For discussion in the framework of the cannonball model see Dado *et al.* (2005).)

The initial fast decaying part of afterglows was argued to be a "sideways" prompt emission, coming from angles $\theta > 1/\Gamma$ (Kumar & Panaitescu, 2000; Barthelmy *et al.*, 2005). If this interpretation is correct, one can determine emission radii of the prompt emission and compare them with model predictions. (We remind that FBM predicts radii of emission $r_{em} \sim 2\Gamma_0^2 c \delta t \sim 10^{12} - 10^{13}$ cm, while EMM predicts $r_{em} \leq r_{dec} \sim 10^{16}$ cm, Eq. 9). If emission is generated at r_{em} and is coming to observer from large angles, $\theta > 1/\Gamma$, its delay with respect to the start of the prompt pulse is $\Delta t \sim (r_{em}/c)\theta^2/2$. For typical observer angle $\theta \sim 0.1$ and first break of a light curve at $\Delta t \sim 1000$ seconds, the implied emission radius is $r_{em} \sim 6 \times 10^{15}$ cm. *This is at least two orders of magnitude larger than is assumed in the fireball model, but is close to the assumption of the electromagnetic model.* [To be consistent with FBM and variability on short times scales, the Lorentz factor of the flow should be $\Gamma_0 \sim 3000$, but this would imply that emission is strongly de-boosted, $\Gamma_0\theta \sim 300 \gg 1$.] *Interpretation of light curves breaks at $\sim 10^3$ s as been due to prompt emission seen at large angles, $\theta > 1/\Gamma$, is inconsistent with the fireball model.*

10.4. Fast variability from large radii

If prompt emission is produced at distances $\sim 10^{15} - 10^{16}$ cm, how can fast variability, on times scales as short as milliseconds, be achieved? One possibility, is that emission is beamed in the outflow frame, for example due to relativistic motion of "fundamental emitters" (Lyutikov & Blandford, 2003). Possible origin of relativistic motion of "fundamental emitters" may be the fact that in case of relativistic reconnection occurring in plasma with $\sigma \gg 1$, the outflowing matter reaches relativistic speeds with $\gamma_{out} \sim \sigma$ (Lyutikov & Uzdensky, 2003). Internal synchrotron emission by such jets, or Compton scattering of ambient photons will then be strongly beamed in the frame of the outflow.

Consider an outflow moving with a bulk Lorentz factor Γ with randomly distributed emitters moving with respect to the shell rest frame with a typical Lorentz factor γ_T . Highly boosted emitters, moving towards an observer, have Lorentz factor $\gamma \sim 2\gamma_T\Gamma$, so that modest values of $\gamma_T \sim 5 - 10 \ll \Gamma \sim 100 - 300$ suffice to produce short time scale variability from large distances. As the burst progresses, larger angles and more of internal jets producing prompt emission become visible. Most of them will be seen from large angles $> 1/\gamma_T$ in the bulk frame, producing smooth curves. Occasionally, a jet at large viewing angle, $\theta > 1/\Gamma$, but directed towards an observer will be seen, producing an X-ray flare. One expects a break in the light curve at $\Delta t \sim (r_{em}/c)\theta^2/2$, where θ is a viewing angle (in a structured jet model, this is the angle between the jet axis and direction to the observer). Afterglow should start to blend with prompt emission at later times. In Fig. A4 we plot an example of a prompt light curve in this model (Lyutikov, in prog.). The model readily explains many unusual properties of early afterglows: (i) X-ray flares and light curve breaks at late times, much longer than conventional prompt GRB duration (extended source activity is not needed!), (ii) fast variability, (iii) gradual softening of the spectrum, (iv) hardening of a spectrum during

X-ray flares (Burrows *et al.*, 2005).

10.5. Observational implications of the electromagnetic model

In this section we give a short discussion of how the main GRB phenomena are (or may be) explained within a framework of EMM.

- **Jet break in afterglow** GRB outflows have large opening angles, but do not have a jet in a proper sense. Outflows are non-isotropic so an achromatic break is inferred when the viewing angle is $\theta_{ob} \sim 1/\Gamma$.
- **Structured jet.** The model predicts and gives a theoretical foundation for the “structured jet” profile of the external shock.
- **XRF flashes.** Another testable prediction of the model is that much more numerous X-ray flashes (XRFs) should be observed, which may be coming “from the sides” of the expanding shell, where the flow is less energetic and the Lorentz boosting is weaker. In addition, the total *bolometric* energy inferred for XRFs (from observations of afterglows before radiative losses become important) should be comparable to the total bolometric energy of γ -ray bursts. Generally, the distributions of parameters of XRFs should continuously match those of GRBs.
- **Weak thermal precursor.** If a fraction $1/\sigma \sim 0.01 - 0.1$ of the magnetic energy is dissipated near the source, this should produce a thermal precursor with luminosity $\sim 0.01 - 0.1$ of the main GRB burst.
- **Hard-soft evolution .** The trend of GRB spectra to evolve from hard to soft during a pulse is explained as a synchrotron radiation in an expanding flow with magnetic field decreasing with radius $B \propto \sqrt{L}/r$ (later in a pulse emission is produced further out where magnetic field is weaker, so that the peak energy will be lower; this is similar to “radius-to-frequency mapping” in radio pulsars and AGNs).
- **Amati $E_{peak} - L$ correlation.** A correlation between peak energy and total luminosity, $E_{peak} \sim \sqrt{L}$ (Amati *et al.*, 2002) follows from the assumption of a fixed typical emission radii and fixed minimum particle energy since $B \sim \sqrt{L_\Omega}$.
- **Variability.** Variability of the prompt emission reflects the statistical properties of dissipation (and not the source activity as in the FBM). Magnetic fields are non-linear dissipative dynamical system which often show bursty behavior with power law PDF. [For example, solar flares show variability on a wide range of temporal scales, down to minutes, which are unrelated to the time scale of 22 years of magnetic field generation in the tachocline.]
- **Prompt and afterglow polarization.** Claims of high polarization (Coburn & Boggs, 2003; Willis *et al.*, 2005) if confirmed, may provide a decisive test of GRB models (see though Rutledge & Fox, 2003). The best way to produce polarization in the range $10\% \leq \Pi \leq 60\%$ is through synchrotron emission in large scale magnetic fields (Lyutikov *et al.*, 2003). (Larger polarization can only be pro-

duced with inverse Compton mechanism, smaller polarization can be produced by small scale magnetic fields.)

Large scale field structure in the ejecta emission may also be related to polarization of afterglows if fields from the magnetic shell are mixed in with the shocked circumstellar material. In this case, *the position angle should not change through the afterglow* while if polarization is observed both in prompt and afterglow emission the position angle should be the same. Also, polarization should be most independent of the "jet break" moment.

11. Conclusion

In this contribution I outlined the underlying assumptions for the "electromagnetic hypothesis" for ultra-relativistic GRB outflows. The most striking implications of the electromagnetic hypothesis is that particle acceleration in the sources is due to direct dissipation of electromagnetic energy rather than shocks and that the outflows are cold, electromagnetically dominated flows, at least until they become strongly dissipative.

One of the major drawback of the model is that magnetic dissipation and particle acceleration are very complicated processes, depending crucially on the kinetic and geometric properties of the plasma. This situation may be contrasted with the shock acceleration schemes, where a qualitatively correct result for the spectrum of accelerated particles, *a kinetic property*, can be obtained from simple *macroscopic* considerations (jump conditions). Example of the Solar corona shows that despite being complicated magnetic dissipation is an effective mean of particle acceleration.

I have discussed possible observational tests of the hypothesis. In particular, interpretation of early afterglow features as being due to prompt emission seen at large angles, $\theta \geq 1/\Gamma$, allows to measure radius at which prompt emission has been produced. Large prompt emission radii, $\sim 6 \times 10^{15}$ cm seem to be inconsistent with the fireball model, but close to prediction of the electromagnetic model. Internal relativistic motion of "fundamental emitters" assumed within EMM may also explain X-ray flares during early afterglow phases (without a need for long source activity). An important implication of the electromagnetic model is that supernova explosions may be magnetically driven as well (Leblanc & Wilson, 1971; Bisnovatyi-Kogan, 1971; Wheeler *et al.*, 2005; Proga *et al.*, 2003).

Over the years I have benefited from discussion with many colleagues, too numerous to be named here. In preparing this contribution I am grateful to Roger Blandford, Tomas Janka, Davide Lazzati, Ehud Nakar, Maurice van Putten and Stephan Rosswog for discussions and comments. I am also indebted to Robert Mochkovitch for shearing his unpublished results.

References

Aloy, M. A. and Janka, H.-T. and Müller, E., 2005, A&A, 436, 273

- Amati, L *et al.*, 2002, A&A, 390, 81
- Barthelmy, S. D., *et al.* 2005, astro-ph/0511576
- Beloborodov, A. M., 2002, ApJ, 565, 808
- Benz, A. O., Saint-Hilaire, P., 2003, Advances in Space Research, 32, 2415
- Bisnovatyi-Kogan, G. S., 1971, Soviet Astronomy, 14, 652
- Blackman, E. G., Field, G. B., 1994, Physical Review Letters, 73, 3097
- Blandford, R. D. & McKee, C. F. 1976 Phys. Fluids 19 1130
- Blandford, R. D. 2002 Lighthouses of the Universe ed. R. Sunyaev Berlin:Springer-Verlag
- Boër, M. and Atteia, J. L. and Damerdji, Y. and Gendre, B. and Klotz, A. and Stratta, G., Submitted to Nature, astro-ph/0510381
- Bogovalov, S., 2001, A&A, 371, 1155
- Burrows, D. N. *et al.*, 2005, astro-ph/0511039
- Chincarini, G. *et al.*, 2005, astro-ph/0511107
- Covino, S., Antonelli, L.A., Romano, P., *et al.* 2005a, GCN Circ. 3665
- Chiueh, T., Li, Z-Y. & Begelman, M., 1991, ApJ, 377, 462,
- Coburn, W., & Boggs, S.E. 2003, Nature, 423, 415
- Craig, I. J. D., Litvinenko, Y. E., 2002, ApJ, 570, 387
- Dado, S. and Dar, A. and De Rujula, A., astro-ph/0512196
- De Villiers, J.-P. and Hawley, J. F. and Krolik, J. H. and Hirose, S., 2005, ApJ, 620, 878
- Daigne, F. & Mochkovitch, R., 2002, MNRAS, 336, 1271
- Djorgovski, S. G. and Kulkarni, S. R. and Bloom, J. S. and Goodrich, R. and Frail, D. A. and Piro, L. and Palazzi, E. , 1998, ApJ, 508, 17
- Drenkhahn, G. and Spruit, H. C., 2002, A&A, 391, 1141
- Fenimore, E. E. and Madras, C. D. and Nayakshin, S., 1998, ApJ, 473, 998
- Ferrari, A., 2004, Ap&SS, 293, 15
- Fox, D. B, *et al.*, Nature in press, astro-ph/0510110
- Ghirlanda, G. and Celotti, A. and Ghisellini, G., 2003, A&A, 406, 879
- Gehrels, N., Barbier, L., Barthelmy, S.D., *et al.* 2005, Nature 437, 851
- Goldreich, P., Julian, W. H., 1970, ApJ, 160, 971
- Hawley, J. F. and Krolik, J. H., 2005, astro-ph/0512227
- Heyvaerts, J. & Norman, C. 2003, accepted for publication in ApJ, astro-ph/0309132
- Hjorth, J. *et al.*, 2003, Nature, 423, 847
- Kennel, C. F., & Coroniti, F. V. 1984a, ApJ, 283, 694
- Klotz, A., 2005, A&A, 439, 35
- Kobayashi, S., 2000, ApJ, 545, 807

- Kompaneets A.S., 1960, Sov. Phys. Doklady, 130, 1001
- Kouveliotou, C., Meegan, C. A., Fishman, G. J., Bhat, N. P., Briggs, M. S. *et al.*s, 1993 ApJ, 413, 101
- Kumar, P., & Panaitescu, A. 2000, ApJ Lett., 541, 51
- Landau, L. D. and Lifshits, E. M., 1982, "The electrodynamics of continuous media (2nd revised and enlarged edition)", Pergamon Press
- Larrabee, D. A., Lovelace, R. V. E., Romanova, M. M. , 2003, ApJ, 586, 72
- Lazzati, D. and Begelman, M., 2005, astro-ph/0511658
- Leblanc, J. M., Wilson, J. R., 1970, ApJ, 161, 541
- Liang, E., Nishimura, K., 2003, arXiv:astro-ph/0308301
- Lipunov, V. M. and Postnov, K. A. and Prokhorov, M. E. , 2001, Astronomy Reports, 45, 236
- Lyutikov, M. & Usov, V. V., 2000, ApJ, 543, 129
- Lyutikov, M., 2002, Phys. Fluids, 14, 963
- Lyutikov, M., 2003, MNRAS, 346, 540
- Lyutikov M., Blandford R., 2003, astro-ph/0312347
- Lyutikov, M., Uzdensky D., 2003, ApJ, 589, 893
- Lyutikov, M., Pariev, V., Blandford, R., 2003, ApJ, 597, 998
- Lyutikov, M., 35th COSPAR Scientific Assembly, p237, astro-ph/0409489
- MacFadyen, A. I. and Woosley, S. E. and Heger, A., 2001, ApJ, 550, 410
- McKinney, J. C. and Gammie, C. F., 2004, ApJ, 611, 977-995
- McMahon, E. and Kumar, P. and Piran, T., 2005, astro-ph/0508087
- Medvedev, M. V. and Loeb, A., 1999, ApJ, 526, 697
- Nakar, E. and Piran, T., 2002, MNRAS, 330, 920
- Nakar, E. and Piran, T., 2004, MNRAS, 353, 647
- Nousek, J. A. *et al.*, 2005, astro-ph/0508332
- Piran, T., 2004, The Physics of Gamma-Ray Bursts, astro-ph/0405503
- Prochaska, J.X., *et al.* 2005, submitted to ApJL, astro-ph/0510022
- Proga, D., MacFadyen, A. I., Armitage, P. J., Begelman, M. C., 2003, astro-ph/0310002
- Rees, M. J., Gunn, J. E., 1974, MNRAS, 167, 1
- Retter, A., Barbier, L., Barthelmy, S., *et al.* 2005, GCN Circ. 3788
- Rossi, E., Lazzati, D., Rees, M. J., 2002, MNRAS, 332, 945
- Rosswog, S. and Ramirez-Ruiz, E. and Davies, M. B., 2003, MNRAS, 345, 1077
- Ruffert, M. and Janka, H.-T., 2001, A&A, 380, 544
- Rutledge, R., Fox, D., 2003, astro-ph/0310385
- Sari, R. and Piran, T., 1999, ApJ, 520, 641

- Shapiro, P., 1979, ApJ, 233, 831
- Smolsky M.V., Usov V.V. 1996, ApJ, 461, 858
- Stanek, K. Z., Matheson, T., Garnavich, P. M., Martini, P., Berlind, P., 2003, ApJ, 591, 17
- Tagliaferri, G. *et al.*, 2005, Nature, 436, 985
- Thompson, C. & Blaes, O. 1998, Phys. Rev. D, 57, 3219
- Thompson, C., Madau, P., 2000, ApJ, 538, 105
- Usov, V. V., 1992, Nature, 357, 472
- van Putten, M. H. P. M., 2005, astro-ph/0510348
- Villasenor, J.S., *et al.*, 2005, Nature, 437, 855
- Willis, D. R. and Barlow, E. J. and Bird, A. J. and Clark, D. J. and Dean, A. J. and McConnell, M. L. and Moran, L. and Shaw, S. E. and Sguera, V., 2005, A&A, 439, 245
- Wheeler, J. C. and Akiyama, S. and Williams, P. T., 2005, Ap&SS, 298, 3
- Woosley, S. E., Zhang, W., Heger, A., 2003, in "From Twilight to Highlight: The Physics of Supernovae", p. 87
- Woosley, S. and Heger, A., 2005, submitted to ApJ, astro-ph/0508175
- Zenitani, S. and Hoshino, M., 2004, astro-ph/0411373
- Zhang, B. *et al.*, 2005, astro-ph/0508321

Appendix A. Applicability of fluid approach for blast wave

In case of extremely high Lorentz factors of the ejecta (which require even higher values of σ than were assumed in this paper), fluid approximation for interaction of magnetized ejects with ISM may break down. Consider an interface between ejecta and the surrounding medium in its rest frame. As a particle from the surrounding medium enters ejecta, it starts gyrating in magnetic field. If a fraction $\sigma/(\sigma + 1)$ of the source luminosity L is in the form of magnetic field, then the turn angle in rest frame in one dynamical time is

$$\omega'_B t_{exp} \sim \sqrt{\frac{\sigma}{\sigma + 1}} \frac{2e\sqrt{\pi L}}{c^{5/2} m_p \Gamma^3} \quad (\text{A.1})$$

In order to justify fluid approximation this should be larger than unity, which requires

$$\Gamma \leq \left(\frac{\sigma}{\sigma + 1}\right)^{1/4} \left(\frac{4\pi e^2 L}{c^5 m_p^2}\right)^{1/6} \sim 4 \times 10^4 \quad (\text{A.2})$$

for $\sigma \geq 1$. Thus, for any $\Gamma \leq 4 \times 10^4$ an ISM particle can complete a half turn on a time scale short if compared with the expansion time scale. In this case, in laboratory frame momentum of the ejecta will be given to the particles almost instantaneously. For larger Lorentz factors the instantaneous hydrodynamical approximation is not applicable, but

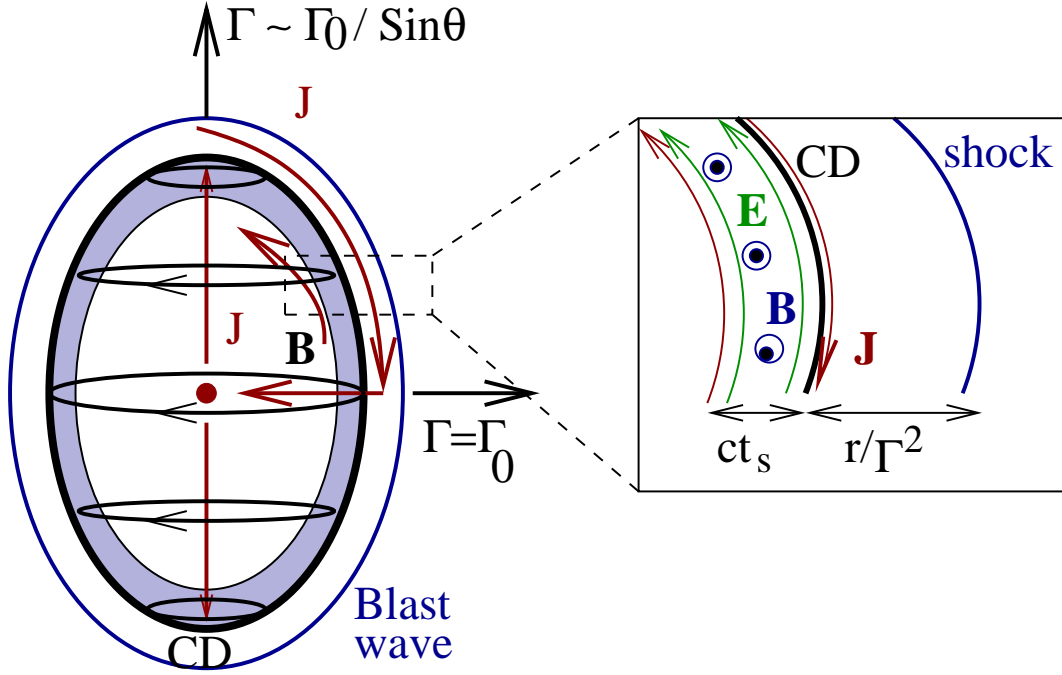


Figure A1. Current flow in the electromagnetic bubble. Current flow mostly along the axis, on the surface of the magnetic shell, along equator and close-up at the trailing part of the shell. Magnetic shell is preceded by the forward shock, typically r/Γ^2 ahead of it. Non-sphericity of the shell, which is of the order $\sim 1/\Gamma^2$, is enhanced.

if particles are turned by an angle larger than $\sim 1/\Gamma$ (larger than $\sim \pi$ in the observer frame) they will still be carried with the flow. Since the rest-frame magnetic field goes as $\sim 1/(t\Gamma(t))$, approximately linearly with time (for constant Γ), the rotational phase of a particle increases only logarithmically, $\int \omega'_B dt' \propto \ln t$. Thus, it takes a very long time for a particle to complete one gyration and be expelled from the ejecta. In this case, the ejecta will be effectively loaded with ISM particles.

Finally, for very high Lorentz factors,

$$\Gamma \geq \left(\frac{\sigma}{\sigma + 1} \right)^{1/4} \frac{\sqrt{e}L^{1/4}}{c^{5/4}\sqrt{m_p}} \sim 8 \times 10^6 \quad (\text{A.3})$$

a particle makes a turn of less than $1/\Gamma$ (in the ejecta frame) on a dynamical times scale. In this case the ejecta just passes through ISM without much interaction and without slowing down.

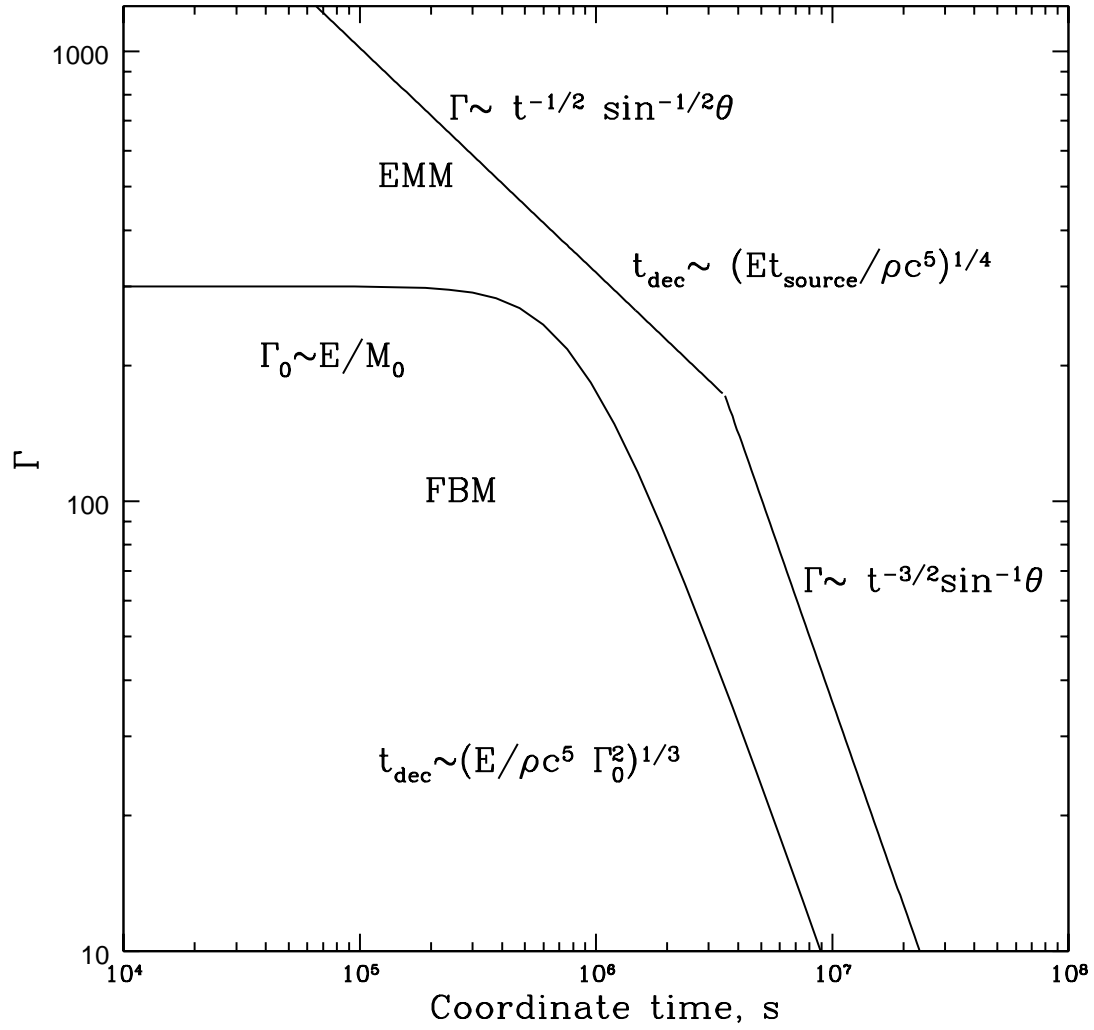


Figure A2. Evolution of Lorentz factors in the fireball and electromagnetic models for constant external density. Relative normalization of the curves depends on the viewing angle (in the EMM).

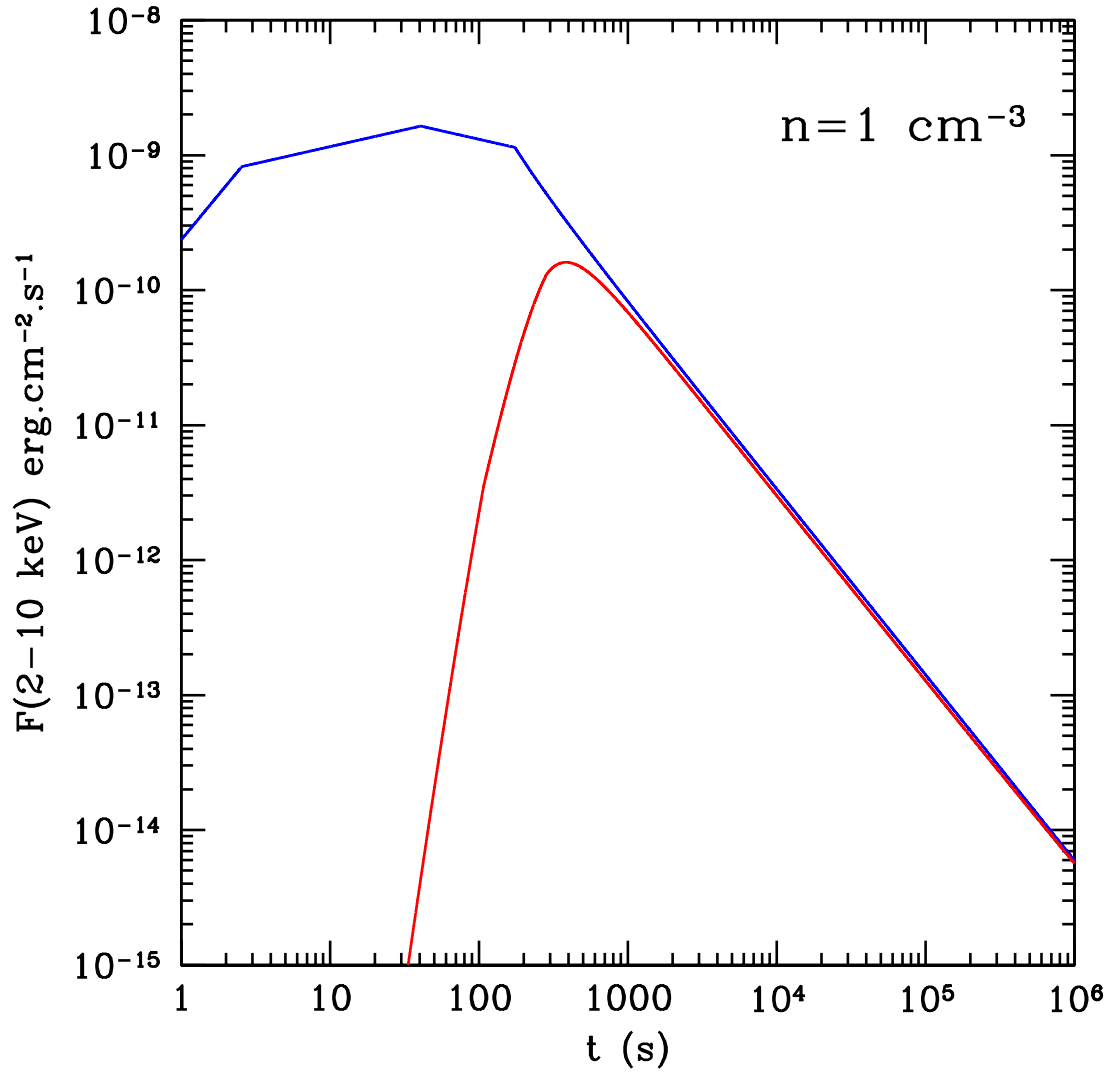


Figure A3. X-ray afterglow in the 2-10 keV energy band for a uniform medium of density $n = 1 \text{ cm}^{-3}$ and injected power $L_{iso} = 10^{52} \text{ erg s}^{-1}$. The source is active for 50 s, the assumed redshift is $z=2.5$, fraction of energy in electrons $\epsilon_e = 0.1$, fraction of energy in magnetic field $\epsilon_B = 0.001$. Blue line: electromagnetic model, red line: fireball model (from Mochkovitch *et al.*, in prep.)

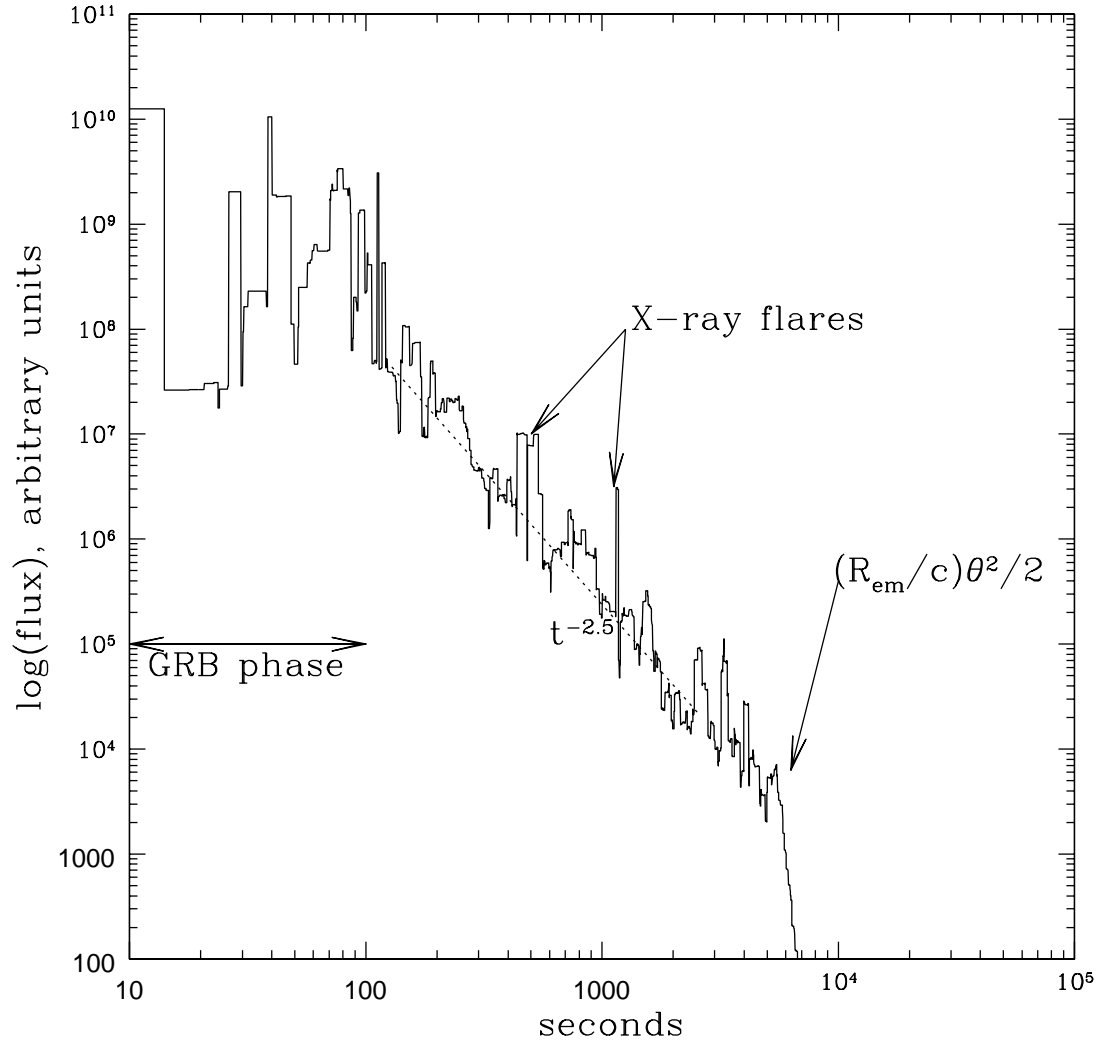


Figure A4. Prompt emission produced by emitters moving randomly in the bulk frame. Emission is generated within a shell of thickness $t_s c = 3 \times 10^{12}$ cm moving with $\Gamma = 100$ at distance $r_{em} = \Gamma^2 t_s c$ by randomly distributed jets with random orientation moving with random Lorentz factors $1 < \gamma_T < \gamma_{T,max} = 5$. Each emitter is active for random time $0 < t'_{em} < 0.5 t_s c \Gamma = t_{pulse,max}$ in its rest frame. Homogeneous jet centered on an observer with opening angle $\theta = 0.1$, dimensionless parameters $N\pi/(\Gamma\gamma_{T,max}\theta)^2 = 1.2$ (probability of seeing one sub-jet "head-on" from angles $< 1/\Gamma$) and $N(ct_{pulse,max}/2)^2/r_{em}^2\theta^2 t_s c \Gamma = 0.19$ (efficiency of energy conversion), where N is total number of emitters. Intensity of emission is $\propto \delta^{3+\alpha}$, where δ is Doppler factor and $\alpha = 0.5$ is spectral index. As the burst progresses, the average Doppler factor $\delta \approx t_s \Gamma/t$ and the average flux decays as $t^{-(2+\alpha)} = t^{-2.5}$ in accordance with analytical estimates (Fenimore *et al.*, 1998) (Lyutikov, in prog.)